Electrochimica Acta 125 (2014) 488–496

Contents lists available at ScienceDirect

Electrochimica Acta

journal homepage: www.elsevier.com/locate/electacta

Preparation and supercapacitance performance of manganese oxide nanosheets/graphene/carbon nanotubes ternary composite film

Qianqiu Tang, Minqiang Sun, Shuangmin Yu, Gengchao Wang*

Shanghai Key Laboratory of Advanced Polymeric Materials, Key Laboratory for Ultrafine Materials of Ministry of Education, School of Materials Science and Engineering, EastChinaUniversity of Science and Technology, Shanghai, 200237, PR China

ARTICLE INFO

Article history:
Received 19 October 2013
Received in revised form 23 January 2014
Accepted 23 January 2014
Available online 8 February 2014

Keywords:
MnO_2 nanosheets
graphene
carbon nanotubes
ternary composite
supercapacitor

ABSTRACT

A novel MnO_2 nanosheets/graphene nanosheets/carboxylic multi-walled carbon nanotubes (MONS/GNS/*c*MWCNT) ternary composite film was fabricated through a filtration-directed self-assembly method. The Field emission scanning electron microscopy (FESEM) and transmission electron microscopy (TEM) images showed the porous sandwiched structure of MONS/GNS/*c*MWCNT with GNS providing a conductive substrate and *c*MWCNT functioning as a vertical electron pathway. The X-ray diffraction (XRD) and Raman spectra further confirmed that the introduction of GNS and *c*MWCNT restricted the serious aggregation of MONS, resulting in a higher specific area (691 m^2g^{-1}). As a result, the MONS/GNS/*c*MWCNT composite film exhibited higher specific capacitance (248 Fg^{-1} at 1 Ag^{-1} in 1 M Na_2SO_4), better rate performance (66.9% capacitance retention from 0.2 to 10 Ag^{-1}) and cycling stability (86.5% retention after 3000 cycles) compared with those of pure dried MnO_2 nanosheets.

1. Introduction

Nowadays, high-performance supercapacitors have become a most important electrochemical energy storage device with their high power output and long cycle life [1–3]. Considerable efforts have been devoted to the development of electrode materials, which are mainly classified into high-surface carbons [4–6], transition metal oxides [7–9], and conducting polymers [10–12]. Among them, manganese dioxide (MnO_2) is one of the most attractive candidates for electrode materials due to its high theoretical specific capacitance (SC) of 1370 Fg^{-1}, low cost, natural abundance and environmental benignity [13–16]. However, densely packed structure, poor intrinsic electrical conductivity and structural instability of MnO_2 seriously restricts the improvement of its practical capacitance, rate capability, and cycling stability, thus limiting its practical application.

As an important strategy to improve the performance of electrode materials, nanostructuring provides more accessible surface area for energy storage and facilitates ion and electron transport [17–20]. Thus up to now, much effort has been devoted to the nanostructuring of MnO_2, including fabricating nanoparticles [21,22], nanowires [23–25], nanorods [26], nanosheets [27–36], nanotubes [37], and nanoflowers [38–40], so as to get enhanced specific capacitance and power delivery capability.

Among various nanostructured MnO_2, colloidal nanosheets of MnO_2 has been synthesized through a simple single-step procedure [27,30,41], which is more convenient and time-saving than previous chemical exfoliation method [42–48]. More importantly, with their unique 2-dimensional structure, MnO_2 nanosheets are promising building blocks to form MnO_2-based nanocomposites with other 0-dimensional, 1-dimensional or 2-dimensional structures such as acetylene black [27], carbon nanotubes [28], graphene [29–31], and conducting polymers [32–34].

The combination of MnO_2 nanosheets with carbonaceous materials is often utilized to enhance the conductivity of MnO_2. However, it often involves the introduction of electrochemical inactive components such as poly(diallyl dimethyl ammonium chloride) (PDDA) and poly(sodium 4-styrenesulfonate) (PSS) in the previous literatures [28–30], imposing negative effects on the specific capacitance of MnO_2-based nanocomposites. For conducting polymer-intercalated layered MnO_2 nanocomposites, these composites often still suffer from relatively poor rate capability and unsatisfactory cycling stability even with remarkable improved capacitance [32–34]. From what we have demonstrated above, the potential of colloidal nanosheets of MnO_2 is far from been exploited due to the lack of delicate structure tailoring on a nano level.

In this paper, we have fabricated a novel composite film based on MnO_2 nanosheets/graphene nanosheets/carboxylic multi-walled carbon nanotubes (MONS/GNS/*c*MWCNT) through a filtration-directed self-assembly method (shown in Scheme 1). The whole preparation process is simple and it does not introduce any electrochemically inert components such as PDDA and PSS. In the ternary

---

* Corresponding author. Tel./Fax: +86 21 64253527.
E-mail address: gengchaow@ecust.edu.cn (G. Wang).

0013-4686/$ – see front matter © 2014 Elsevier Ltd. All rights reserved.
http://dx.doi.org/10.1016/j.electacta.2014.01.139

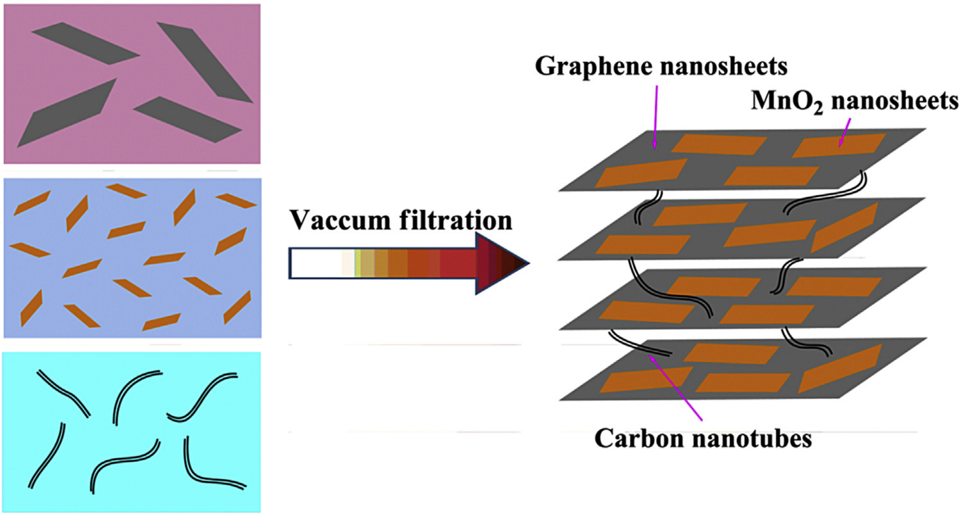

Scheme 1. Schematic illustration of the fabrication of the MONS/GNS/*c*MWCNT ternary composite film.

composite film, GNS provides a conducting substrate with large accessible surface area for MONS to deposit, restricting the dense stacking of MONS, and *c*MWCNT facilitate the vertical flow of electron so as to form a more perfect conducting network. Besides, *c*MWCNT expand the interlayer spacing of MnO_2 nanosheets and graphene, engendering a porous structure with larger surface area for energy storage and electrolyte penetration. Furthermore, both the flexible substrate of GNS and the scaffold of *c*MWCNT exhibit good chemical stability and strong mechanical properties, which can compensate for the volume change of MONS during cycling. Taking full advantage of each component and their synergistic effect, the ternary composite film exhibits improved specific capacitance, rate capability and cycling stability.

2. Experimental

2.1. Preparation of the colloidal suspension of MnO_2 nanosheets (MONS)

The colloidal suspension of MnO_2 nanosheets (MONS) was prepared through a one-pot procedure reported in the previous literature [41]. Typical procedure was as follows: 12 mL 1 M tetramethylammonium hydroxide (TMAOH) and 2 mL 30 wt% H_2O_2 were mixed and diluted to 40 mL by deionized water. Then, the mixed solution was poured to 10 mL 0.3 M $Mn(NO_3)_2$ under vigorous stirring and kept stirring for 12 h at room temperature. The resulting suspension was dialyzed in deionized water until the pH reaches 6~7. Finally, the colloidal suspension of MONS was obtained by using a centrifuge to separate the precipitate at a speed of 5000 rpm.

2.2. Preparation of colloidal suspension of GNS and cMWCNT

Graphite oxide was synthesized from natural graphite with Hummers method [49], The colloidal suspension of graphene nanosheets (GNS) were prepared by directly reducing graphene oxide with hydrazine [50]. Then the suspension of GNS was dialyzed in ammonia aqueous solution to remove hydrazine.

MWCNTs (diameter <8 nm, Chengdu Organic Chemicals Co. Ltd. of Chinese Academy of Sciences) were treated in a mixture of concentrated H_2SO_4 and HNO_3 (3:1 v/v) at 60 °C for 1 h to introduce carboxylic acid groups, achieving a stable suspension of *c*MWCNT [51].

2.3. Fabrication of MONS/GNS/cMWCNT ternary composite film

To fabricate the MONS/GNS/*c*MWCNT ternary composite film, the as-prepared MONS, GNS and *c*MWCNT colloidal suspension were mixed with the mass ratio of 70/25/5. The MONS/GNS/*c*MWCNT ternary composite film was prepared through vacuum filtration of the mixed dispersion with PVDF filter membrane (0.45 μm pore size). For comparison, the MONS/GNS binary composite film was prepared with the mass ratio of 70/30 through the same procedure as above, and MONS/*c*MWCNTs (70/30) was prepared by mixing MONS and *c*MWCNTs dispersion, followed by freezing drying.

2.4. Materials characterization

Atomic Force Microscopy (AFM) images were obtained with a multimode atomic force microscopy (NanoscopeIIIa, Veeco), employing the uncontact mode. The morphologies of the as-prepared samples were observed by field-emission scanning electron microscope (FE-SEM, Hitachi S-4800) and transmission electron microscopy (TEM, JEOL JEM-1400). Powder X-ray diffraction (XRD) patterns were performed in a Rigaku D/Max 2550 VB/PC X-ray diffractometer using Cu (Kα) radiation with the 2θ-angle recorded from 5~70°. The XRD data of MONS was collected with a wet sample, and for all the other materials, dried powder samples were used. Raman spectra were recorded with a Renishaw inVia + Reflex using a 50 mW He – Ne laser operated at 514.5 nm. X-ray photoelectron spectroscopy (XPS) spectra were recorded with a thermo scientific ESCALAB 250Xi X-ray photoelectron spectrometer equipped with a monochromatic Al Kα X-ray source (1486.6 eV). The UV – vis spectra were obtained using a Shimadzu UV-2102PC spectrophotometer. The Zeta potentials of MONS, GNS and *c*MWCNT were measured on Zetasizer Nano-ZS model ZEN 3600 (Malvern, USA). Digital photos were taken by Nikon COOLPIX S6300. The electrical conductivity of the samples was determined using a SX 1934 four-probe instrument.

2.5. Electrochemical measurements

The working electrodes of dried MONS, MONS/*c*MWCNT and *c*MWCNT were prepared by mixing 85% active material, 10%